European Particle Accelerator Conference BNL-67358
Vienna, Austria, June 26-30, 2000

RING RF AND LONGITUDINAL DYNAMICS IN THE SNS*

M. Blaskiewicz, J.M. Brennan, J. Brodowski, J. Delong, M. Meth, E. Onillon, A. Zaltsman
BNL, Upton NY 11973, USA

Abstract

Average beam currents of 40 A will be present in the Spallation Neutron Source. Even though the entire cycle time is only one synchrotron oscillation the longitudinal phase space determines peak beam current and momentum spread. Both factors play a role in space charge and instability dynamics. Longitudinal simulations with beam loading and longitudinal space charge have been done in the design phase.

1 INTRODUCTION

The main purpose of the RF system is to maintain a 250 ns gap for the rise time of the extraction kicker with low peak beam current and large momentum spread[1, 2]. The latter considerations prevent space charge stopband related losses and coherent instabilities. The design philosophy is to err on the side of caution when necessary. This is prudent when dealing with peak currents $\sim$ 100 A and guarantees a system which achieves, and possibly exceeds, the design goals.

The SNS ring has a circumference $C = 248$ m, with a transition Lorentz factor of $\gamma_t = 5.25$. The 1 GeV, H^- linac beam is charge exchange injected, using a stripper foil, for 1100 turns[3]. The 2×10^{14} protons are then extracted using a fast kicker system and sent to the target. The rf design calls for a dual harmonic system with harmonic numbers $h = 1$ and $h = 2$, and with voltage amplitudes of $V_1 = 40$ kV/turn and $V_2 = 20$ kV/turn. The system involves proven technology and generates a bunching factor nearly as good as a barrier cavity system[1, 2].

For small beam currents the RF system generates a low current bucket area of $\epsilon_{bucket} = 19$ eV $-$ s. For a gap of 250 ns the low current bunch emittance is $\epsilon_{bunch} = 13$ eV $-$ s with a full energy spread of ± 11.1 MeV and a synchrotron period of 1400 turns at the edge of the bunch. For high currents the longitudinal space charge impedance reduces the bucket area and maximum energy spread. There are also beam loading effects, which are considered below. With good beam loading compensation a full energy spread of ± 9.8 MeV is typical.

2 CAVITY AND POWER AMPLIFIER

Harmonic numbers of 1 and 2 imply cavity frequencies of $f_1 = 1.05$ MHz and $f_2 = 2.11$ MHz. The $h = 1$ cavities are designed for 10 kV/gap and the $h = 2$ cavities are identical but for less gap capacitance. Phillips 4M2 ferrite is used. Measurements show a peak RF magnetic field of $B_{rf} = 40$ mT can be achieved , with negligible bias, at SNS frequencies and duty cycle. The design assumes $B_{rf} \leq 31$ mT. The inner and outer radii of the ferrite rings are $a = 12.5$ cm and $b = 25$ cm. Assuming the magnetic field varies as $1/r$ the gap voltage is

$$V_{gap} = 2\pi f B_{rf} \ell a \ln(b/a), \qquad (1)$$

where ℓ is the total length of the ferrite stack. The thickness of the ferrite rings is 2.72 cm and 21 are used so $\ell = 57.1$ cm. Setting $V_{gap} = 10$ kV and $B_{rf} = 31$ mT gives $f = 1.05$ MHz. For a beam energy of 800 MeV, as might occur during comissioning, the $h = 1$ frequency is 1.02 MHz and the maximum voltage drops to 9.7 kV/gap for 31 mT. For $h = 1$ the gap capacitance is supplied by four 750 pF units leading to a total gap capacitance $C = 3000$ pF. For $f_{rf} = 1.05$ MHz the required gap inductance is $L_{gap} = 1/\omega_{rf}^2 C = 7.6\mu$H. Since $L_{gap} = \mu_0 \mu_r \ell \ln(b/a)/2\pi$, the required permeability is $\mu_r = 88$. Given the initial permeability of $\mu_r = 130$ a bias current of order 50 A is needed. Ferrite measurements for SNS frequencies and field strengths imply peak loss rates $\sim$ 300 mW/cm^3. This gives a shunt impedance of $R_{gap} = 2$ kΩ with $R_{gap}/Q = 50\Omega$. Each cavity consists of two gaps. The DC bias current flows in opposite directions through the two cells leading to negligible RF voltage across the bias supply.

The design of the power amplifier is driven by beam loading requirements. During the millisecond accumulation the average beam current rises from 0 to 34 A. The maximum amplitude of the first harmonic component is $I_1 = 50$ A and the second harmonic component is down by a factor of 10. The philosophy here is to design the power amplifier for $h = 1$ and use the same design for $h = 2$. This reduces R&D significantly and allows the $h = 2$ system to to be easily modified to $h = 1$ if desired. The base line design requires the power amplifier to fully compensate the beam current while providing the necessary quadrature component to drive the gap voltage. The cavity resonant frequency is fixed, and equal to the RF frequency. In some sense this may be pessimistic but the consequences of this assumption to the overall system cost are not great, whereas the benefits for system performance and reliability are very valuable.

A Thompson (TH558) tetrode drives two gaps in parallel while supplying the necessary anode current. With three cavities (6 accelerating gaps) at $h = 1$ and 7 kV/gap the anode dissipation reaches the tube rating of 600 kW at the end of accumulation. The time average dissipation is much smaller, about 50 kW, but very high reliability is required and stressing the tube could lead to shorter life. The $h = 2$ system has one cavity with two gaps and 10 kV/gap. There

* Work performed under the auspices of the United States Department of Energy

is negligible $h = 2$ beam loading.

3 PHASE AND AMPLITUDE LOOPS

As beam accumulates during the 1 ms cycle its RF current will increase and drive the cavity. The generator voltage phase (ϕ_g) and amplitude (V_g) must vary to maintain the gap voltage phase (ϕ_{gap}) and amplitude (V_{gap}) at the required levels. The detailed design of these loops is ongoing. For estimation purposes take

$$\frac{d\phi_g}{dt} = \frac{\phi_0(t) - \phi_{gap}}{\tau_\phi}, \tag{2}$$

where τ_ϕ is a time constant characterizing the loop's bandwidth and $\phi_0(t)$ is the target cavity phase. The target phase can be derived from the beam, an external clock, or a mixture of both. The amplitude loop is approximated as

$$\frac{dV_g}{dt} = \frac{V_0(t) - V_{gap}}{\tau_a}, \tag{3}$$

where τ_a characterizes the bandwidth of the loop and $V_0(t)$ is the target cavity voltage. Given experience at other machines and simulation work[6], the target voltage will probably ramp up during accumulation.

4 BEAM LOADING AND MACHINE IMPEDANCE

Now that the power requirements and low level control of the RF system are satisfied the stability of the beam cavity interaction must be addressed. The instantaneous gap voltage, generator current (I_g) and beam current (I_b) are related via

$$\begin{aligned} I_g(t) + I_b(t) &= -\frac{V_{gap}(t)}{R_\ell} - C_{cav}\frac{dV_{gap}(t)}{dt} \\ &\quad - \int^{t} \frac{V_{gap}(t')}{L_{cav}} dt', \end{aligned} \tag{4}$$

where R_ℓ is the loaded shunt impedance of the cavity and power amplifier in parallel. The loaded shunt impedance per gap is $R_\ell \approx 600\Omega$ at the end of accumulation. For a rough estimate consider the beam loading parameter $Y = I_1 R_\ell / V_{gap}$. For the SNS $Y \approx 3$ at the end of the cycle and the stability of the system could be compromised[5, 7, 10, 9]. The phase and amplitude loops will help stabilize the system but a beam based feedforward correction is also planned. To reduce radiation exposure and increase reliability, all of the electronics for the digital computatons will reside in the equipment building in the center of the SNS ring. The round trip time for a signal is ≈ 750 ns and the total delay is taken to be about 1.5 turns or 1.4 μs. The cavity and beam pickups are assumed to be broad band but the termination of the grid drive circuit is a $Q = 2$ resonator centered at the RF frequency. Other factors, difficult to estimate, will change the transfer function so the design of the feed forward system includes a narrow band filter around the RF frequency. The net effect of low level loops beam loading and feed forward results in:

$$\begin{aligned} V_{gap}(t) &= V_g(t)\sin[\omega_{rf}t + \phi_g(t)] \\ &\quad + \int_0^\infty d\tau W(\tau) I_T(t-\tau), \end{aligned} \tag{5}$$

$$I_T(t) = I_b(t) - \int_0^\infty d\tau G(\tau) I_b(t - \tau - T_{delay}), \tag{6}$$

where $W(\tau)$ is the wake potential associated with the loaded gap impedance and $G(\tau)$ is a narrow band filter around the RF frequency. For simulations we take a simple filter with spectral representation

$$G(\omega) = \frac{G_0}{1 + jQ_{ff}\left(\frac{\omega}{\omega_{rf}} - \frac{\omega_{rf}}{\omega}\right)}. \tag{7}$$

The RF simulation uses standard techniques[8]. Equations (2) through (6) with filter (7) are transformed into a set of first order differential equations and discretized. The total RF kick is updated once per particle per turn with ~ 50 time slices per turn.

Space charge makes a significant contribution to the longitudinal force. For frequencies below $f_{rf}^2/4\pi h f_s \sim 75$ MHz the space charge forces can be updated once per turn. We neglect these high frequencies and use a single space charge kick per turn. At the reference azimuth the voltage due to space charge is

$$V_{sc}(t) = \frac{Z_{sc}}{\omega_0}\frac{dI_b(t)}{dt}, \tag{8}$$

where $Z_{sc} \approx 200\Omega$ is the space charge impedance[11]. A fast pairwise sum with a smoothing length of 50 ns is used to obtain the total kick[2, 12].

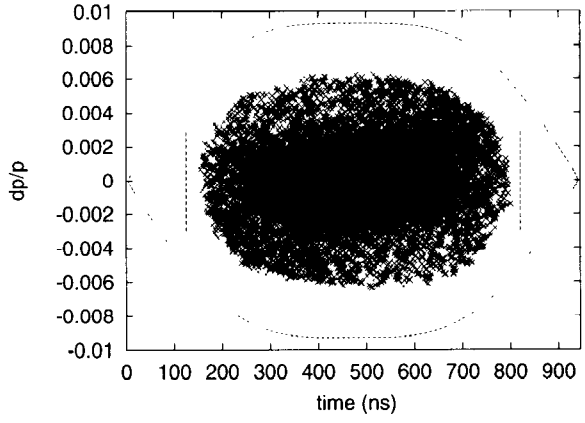

Figure 1: Longitudinal phase space just before extraction

Table 1 summarizes the RF parameters. Notice that the injected energy spread is ± 3.8MeV with a rectangular distribution. This is created by an energy wiggler cavity running at a slightly different frequency from the LINAC RF.

Table 1: RF and Simulation Parameters

parameter	value
circumference	248m
transition gamma	5.25
total h=1 voltage	40 kV
total h=2 voltage	20 kV
space charge Z/n	i200 Ω
proton kinetic energy	1 GeV
injected bunch length	610 ns
injected energy spread	±3.8MeV, full
protons at extraction time	2.08×10^{14}
R_ℓ total $h = 1$	4.0 kΩ
R/Q total $h = 1$	300Ω
G_0	1
$\tau_\phi = \tau_a$	50 μs
macro-particle length; space charge	50 ns
bin size for RF calculations	$T_{rev}/50$
macro-particles added per turn	10
number of turns	1100
output	
rms extracted energy spread	4.0 MeV
maximum bunch length	650 ns
peak beam current	72 A

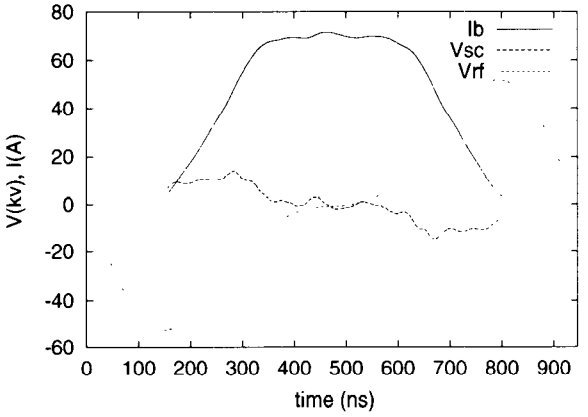

Figure 2: Voltages and currents just before extraction for nominal parameters

The net effect is to broaden the rms width of the energy distribution without creating the tails associated with a debuncher cavity.

For the simulation the $h = 1$ RF voltage was ramped from 30 to 40 kV over the first 500 turns. The $h = 2$ voltage was half the $h = 1$ value throughout. The reference value for the phase loop was 180° and the injected beam was centered with respect to this reference clock. Figure 1 shows the longitudinal phase space, the rf bucket, and the edges of the kicker gap just before extraction. Figure 2 shows the bunch current, the space charge voltage and the total RF voltage just before extraction.

The phase and amplitude loops are necessary, but the RF system is robust with respect to feed forward errors. Figure 3 illustrates the situation when there is no feed forward. The maximum error in the RF voltage waveform is $\lesssim 10$ kV and the bunch is acceptable. Even with marginal feed forward operation the system performace should easily meet its specifications.

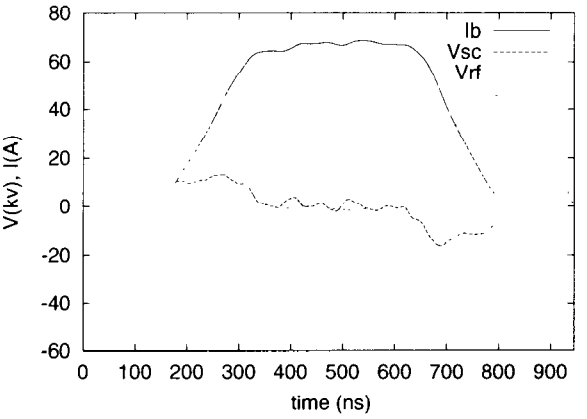

Figure 3: Voltages and currents just before extraction for no feed forward

ACKNOWLEDGEMENTS

Many people have contributed to this work. In particular we thank D. Boussard, Y.Y. Lee, D. Raparia, K. Rogers, R. Spitz, and R. Sanders.

REFERENCES

[1] M. Blaskiewicz, J.M. Brennan, Y.Y. Lee SNS tech note # 9, (1996).

[2] M. Blaskiewicz, J.M. Brennan, A. Zaltsman SNS tech note # 36, (1997).

[3] J. Wei, *these proceedings*

[4] National Spallation Neutron Source, Conceptual Design Report, 4-64, (1997).

[5] F. Pederson, IEEE, TNS, Vol. NS-22, No. 3, pg 1906, (1975).

[6] J. Galambos, ORNL/SNS Technical memo, Nov. (1999)

[7] S. Koscielniak, 5th European Particle Accelerator Conference,pg 1129, 1996.

[8] S. Koscielniak, TRI-DN-97 (1997) *and references therein*

[9] D. Boussard, CERN 91-04 (1991).

[10] R. Garoby, Fontiers of Particle Beams: Intensity Limitations, US-CERN School on Particle Accelerators, Springer-Verlag, pg 509, (1990).

[11] S.Y. Zhang, SNS Tech Note # 43 (1999).

[12] M. Blaskiewicz, *PRST-AB* 044201, (1998).